




RESEARCH ARTICLE

OH reaction rate coefficients, infrared spectra, and climate metrics for (*E*)- and (*Z*)- 2-perfluoroheptene (2-C₇F₁₄) and 3-perfluoroheptene (3-C₇F₁₄)

Aparajeo Chattopadhyay^{1,2}  | Vassileios C. Papadimitriou^{1,2,3}  | James B. Burkholder¹ 

¹Chemical Sciences Laboratory, National Oceanic and Atmospheric Administration, Boulder, Colorado, USA

²Cooperative Institute for Research in Environmental Sciences, University of Colorado, Boulder, Colorado, USA

³Laboratory of Photochemistry and Chemical Kinetics, Department of Chemistry, University of Crete, Heraklion, Crete, Greece

Correspondence

James B. Burkholder, Chemical Sciences Laboratory, National Oceanic and Atmospheric Administration, 325 Broadway, Boulder, CO 80305-3328, USA.
 Email: James.B.Burkholder@noaa.gov

Abstract

In this work, perfluoroheptene 2- and 3-C₇F₁₄ stereoisomer specific gas-phase OH reaction rate coefficients, *k*, were measured at 296 K in ~600 Torr (He bath gas) using a relative rate (RR) method. Gas-chromatography (GC) with electron capture detection (ECD) was used for the separation and detection of the stereoisomers. Rate coefficients for (*E*)-2-C₇F₁₄, (*Z*)-2-C₇F₁₄, (*E*)-3-C₇F₁₄, and (*Z*)-3-C₇F₁₄ were measured to be (in units of 10⁻¹³ cm³ molecule⁻¹ s⁻¹) (3.60 ± 0.51), (2.22 ± 0.21), (3.43 ± 0.47), and (1.48 ± 0.19), respectively, where the uncertainties include estimated systematic errors. Rate coefficients for the (*E*)- stereoisomers were found to be systematically greater than the (*Z*)- stereoisomers by a factor of 1.6 and 2.3 for 2-C₇F₁₄ and 3-C₇F₁₄, respectively. Atmospheric lifetimes with respect to OH radical reaction for (*E*)-2-C₇F₁₄, (*Z*)-2-C₇F₁₄, (*E*)-3-C₇F₁₄, (*Z*)-3-C₇F₁₄ were estimated to be ~33, ~56, ~36, and ~86 days, respectively, for an average OH radical concentration of 1 × 10⁶ molecule cm⁻³. Quantitative infrared absorption spectra were measured as part of this work. Complimentary theoretically calculated infrared absorption spectra using density functional theory (DFT) are included in this work. The theoretical spectra were used to evaluate stereoisomer climate metrics. Radiative efficiencies (adjusted) and global warming potentials (GWPs, 100-year time-horizon), were estimated to be 0.12, 0.19, 0.12, and 0.23 W m⁻² ppb⁻¹ and 1.9, 5.1, 2.1, 9.3 for (*E*)-2-C₇F₁₄, (*Z*)-2-C₇F₁₄, (*E*)-3-C₇F₁₄, (*Z*)-3-C₇F₁₄, respectively. Atmospheric degradation mechanisms are discussed.

KEYWORDS

atmospheric lifetime, greenhouse gases, OH kinetics, perfluoroolefins (PFOs), replacement compounds

1 | INTRODUCTION

Perfluoroolefins (PFOs) are next generation replacement compounds for ozone depleting substances (ODS) and greenhouse gases that are currently in commercial use¹

as refrigerants and foam blowing agents. In general, the goal of a replacement compound is to reduce the ozone depletion potential (ODP) and their climate impact as a greenhouse gas. PFOs are not ODS as they do not contain Cl atoms, but are expected to be potent

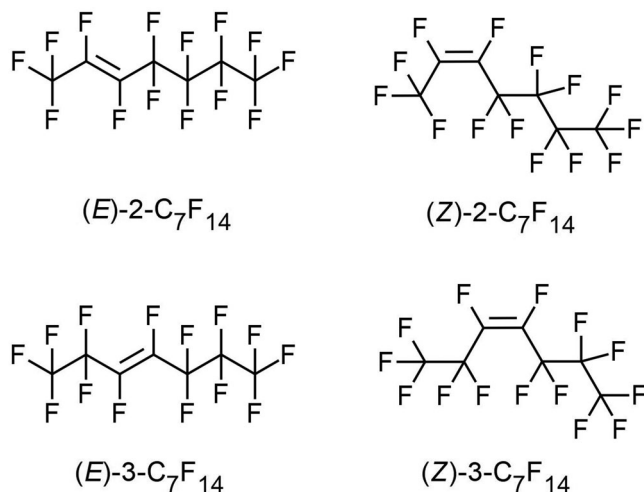


FIGURE 1 (E) and (Z) stereoisomers of 2-C₇F₁₄ and 3-C₇F₁₄.

greenhouse gases. The presence of unsaturated bonds, >C=C<, in PFOs greatly enhances their reactivity toward atmospheric oxidants such as the OH radical and Cl atom over that of saturated perfluorinated compounds, that is, leading to shorter atmospheric lifetimes and lower global warming potentials (GWPs). A quantitative analysis of atmospheric lifetimes, climate metrics, and degradation mechanisms for these compounds are needed for policy-makers to make informed decisions about replacement compounds.

2-perfluoroheptene (2-C₇F₁₄) and 3-perfluoroheptene (3-C₇F₁₄) (Figure 1) are PFOs proposed as potential replacement compounds for perfluorocarbons and hydrofluoroethers in heat transfer applications. Commercial samples of 2-C₇F₁₄ and 3-C₇F₁₄ contain a mixture of (E)- and (Z)- stereoisomers. Reaction of 2-C₇F₁₄ and 3-C₇F₁₄ with the OH radical is expected to be the dominant loss process for these compounds in the atmosphere. To the best of our knowledge, there are no OH radical kinetic studies in the literature for 2-C₇F₁₄ and 3-C₇F₁₄:



and



There is limited kinetic data available for the relative reactivity of stereoisomers. However, studies have demonstrated that stereoisomers can have significantly

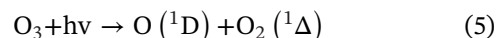
different reactivity with the OH radical.²⁻⁹ In this study, rate coefficients, *k*, for the OH radical reaction with the stereoisomers of 2-C₇F₁₄ and 3-C₇F₁₄ were measured at 296 K using a relative rate method with gas-chromatography-mass spectroscopy (GC-MS) and electron capture (GC-EC) detection of the stereoisomers. As part of this work, complementary absolute rate coefficient measurements were obtained for the commercial stereoisomer mixtures using a pulsed laser photolysis-laser induced fluorescence (PLP-LIF) method. Infrared absorption spectra were also measured for the stereoisomer mixture samples. Theoretically calculated vibrational spectra, at the B3LYP/6-31G(d) level of theory, were used to derive stereoisomer specific the radiative efficiency and GWP climate metrics. A proposed atmospheric degradation mechanism for 2-C₇F₁₄ and 3-C₇F₁₄ following the addition of the OH radical to >C=C< double bond is presented.

2 | EXPERIMENTAL DETAILS

2.1 | Relative rate technique

The details of the RR reactor and the method have been described previously.^{10,11} Briefly, the apparatus consisted of (1) a ~250 cm³ cylindrical Pyrex reactor fitted with quartz windows, (2) a Teflon diaphragm pump used to circulate gases between the reactor and a Fourier transform infrared (FTIR) spectrometer with a White multi-pass gas absorption cell, (3) a KrF excimer laser used for OH radical production, and (4) a GC with MS or EC detection used for stereoisomer measurement.

OH radicals are generated by the 248 nm pulsed KrF excimer laser photolysis of O₃ in the presence of excess H₂O vapor:



Note that 2-C₇F₁₄ and 3-C₇F₁₄ photolysis at 248 nm is negligible in this system.

The loss of the stereoisomers due to OH radical reaction was measured relative to a reference compound. Reaction rate coefficients were determined using the following equation:

$$\ln \left(\frac{S_0}{S_t} \right) = \frac{k}{k_{\text{Ref}}} \ln \left(\frac{R_0}{R_t} \right) \quad (7)$$

$$\ln \left(\frac{[\text{C}_7\text{F}_{14}]_0}{[\text{C}_7\text{F}_{14}]_t} \right) = \frac{k}{k_{\text{Ref}}} \ln \left(\frac{[\text{Ref}]_0}{[\text{Ref}]_t} \right) \quad (8)$$

where S_0 , S_t , are measured GC peak heights for C_7F_{14} stereoisomer at time 0 and time t , respectively, R_0 , R_t are measured GC peak heights for reference compound at time 0 and time t , respectively, $[C_7F_{14}]_0$ and $[C_7F_{14}]_t$ and $[Ref]_0$ and $[Ref]_t$ are the concentrations of a C_7F_{14} isomer and the reference compound at time 0 and t , respectively. (*E*)-(CF₃)₂CFCH = CHF ((*E*)-HFO-1438ezy) and (*E*)-CF₃CF = CFCF₃ were used as reference compounds in this study with recommended OH radical rate coefficients of $(3.26 \pm 0.26) \times 10^{-13} \text{ cm}^3 \text{ molecule}^{-1} \text{ s}^{-1}$,¹¹ and $(4.34 \pm 0.45) \times 10^{-13} \text{ cm}^3 \text{ molecule}^{-1} \text{ s}^{-1}$,³ respectively. These unsaturated reference compounds were chosen for their rate coefficients being similar to the C_7F_{14} stereoisomers and also because of their high EC sensitivity.

Experiments were performed by adding the perfluoroheptene sample, reference compound, and H₂O vapor to the reactor and adjusting the system to a total pressure of ~600 Torr with added He bath gas. A FTIR spectrum and a GC chromatogram were recorded for the initial mixture. A slow flow of He gas which is passed through a 195 K silica-gel trap containing O₃ was added to the reactor for ~10–60 s while the laser was on. Over the course of an entire experiment the total pressure increased ~30–40 Torr due to the O₃/He addition. After the O₃ flow was stopped, a FTIR spectrum and a GC chromatogram were recorded. This process was repeated 5–7 times. The initial concentrations of $[C_7F_{14}]$ (total concentration of (*E*)- and (*Z*)-stereoisomers), $[(E)-(CF_3)_2CFCH = CHF]$, $[(E)-CF_3CF = CFCF_3]$, and $[H_2O]$ were in the range (0.4–4.5) $\times 10^{14}$, $(1.2\text{--}3.1) \times 10^{14}$, $(3.9\text{--}4.3) \times 10^{14}$, and $\sim 2 \times 10^{17}$ molecule cm⁻³, respectively, over the course of the study. The laser was operated at 10 Hz with fluences in the range (0.3–1.1) mJ cm⁻² pulse⁻¹ over the course of the study. The initial OH radical concentration per laser pulse was estimated to be in the range $(2\text{--}14) \times 10^{10}$ molecule cm⁻³.

FTIR spectroscopy was used to measure the initial concentration of total C_7F_{14} . The evolution of each C_7F_{14} stereoisomer and the reference compound during the course of OH reaction was monitored by gas chromatography. The GC was equipped with a RTX1 column (105 m \times 250 μm \times 1 μm). A standard split-splitless GC inlet was maintained at 75°C and operated in split mode with 5:1 split ratio. Column flow, septum purge flow, and split flow were 2.5, 6, and 12.5 cm³ min⁻¹, respectively. The GC oven temperature was programmed to start at -30°C for 1 min, a temperature ramp of 6°C per min until reaching 40°C, a second temperature ramp of 40°C per min up to 260°C, and was held at 260°C for 12 min. The ECD was maintained at 300°C. A small volume (9 μL) of the reaction mixture was extracted for the reactor using a gas-tight syringe and injected into the GC sample port. Representative chromatograms are shown in the support-

ing information, Figures S1–S6. The sample and reference compound kinetics were analyzed based on the isolated GC peak heights. The detection limit of C_7F_{14} by ECD was $\sim 1 \times 10^{10}$ molecule cm⁻³.

2.2 | Infrared absorption spectra

Infrared absorption spectra were measured using a FTIR spectrometer coupled to a multi-pass absorption cell (volume ~500 cm³) fitted with KBr or Ge windows. The optical pathlength was set at 425 cm and spectra were recorded with 1 cm⁻¹ resolution. Absorption spectra were determined using Beer's law with spectra measured over a range of concentrations in a static absorption cell fill. Sample concentrations were determined from the mixing ratio (0.035%–0.046%) of manometrically prepared mixtures in a He bath gas and the measured pressure using the ideal gas law. The spectrum reported here was recorded in ~600 Torr He bath gas.

2.3 | Materials

He (UHP, 99.999%), N₂ (UHP, 99.99%), CF₃CF = CFCF₃ (70% (*E*)- and 30% (*Z*)- stereoisomer mixture), (*E*)-(CF₃)₂CFCH = CHF ((*E*)-HFO-1438ezy) (99.7% purity) samples were used as supplied. Two commercial C_7F_{14} samples were used with the following quoted sample compositions: (1) 2- C_7F_{14} ((*E*)-2- C_7F_{14} = 84.95%, (*Z*)-2- C_7F_{14} = 10.82%, (*E*)-3- C_7F_{14} = 1.72%, (*Z*)-3- C_7F_{14} = 0.79%), (2) 3- C_7F_{14} ((*E*)-2- C_7F_{14} = 1.19%, (*Z*)-2- C_7F_{14} = 0.03%, (*E*)-3- C_7F_{14} = 95.98%, (*Z*)-3- C_7F_{14} = 1.18%). The remaining fractions were primarily other perfluoroheptenes (~1.5%) with a minor impurity (0.1%–0.3%) not identified. The C_7F_{14} samples were degassed by several freeze-pump-thaw cycles and dilute mixtures in either He or N₂ bath gas were prepared manometrically in 12 L Pyrex bulbs. Distilled H₂O was degassed prior to use. O₃ was generated by flowing O₂ through an ozonizer and was collected at ~195 K in a silica gel trap. Concentrated H₂O₂ (~95%) used in the PLP-LIF measurements was prepared by bubbling N₂ through a ~65% sample. A COF₂ infrared absorption spectrum was recorded using a commercially obtained sample.

3 | THEORETICAL CALCULATIONS

Quantum mechanical molecular calculations were employed to calculate infrared absorption spectra for the (*E*)- and (*Z*)- C_7F_{14} isomers included in this work using density functional theory (DFT) methods and the Gaussian 16 software package suite. In particular, the

stereoisomer geometries were optimized using the B3LYP functional in conjunction with basis sets of double- ζ quality (6-31G(d)) and applying tight convergence criteria and UltraFine integration grid. Anharmonic frequencies, overtones and combination bands were calculated at the B3LYP/6-31G(d) level of theory, via numerical differentiation including vibrational-rotational (*VibRot*) coupling. The theoretically obtained vibrational band stick-spectra were further processed using a Gaussian broadening function, FWHM = 20 cm⁻¹, for comparison with the experimental spectra of the C₇F₁₄ stereoisomer mixtures.

4 | RESULTS AND DISCUSSION

The sections below describe (1) the measured rate coefficients for reactions 1–4 at 296 K using a relative rate method at ~600 Torr (He) pressure; (2) complementary absolute rate measurements for the 2-C₇F₁₄ and 3-C₇F₁₄ samples using a pulsed laser photolysis-laser-induced fluorescence (PLP-LIF) method; (3) O₃ reaction rate coefficients; (4) Infrared absorption spectrum measurements of the 2-C₇F₁₄ and 3-C₇F₁₄ samples, which contain a mixture of (*E/Z*) stereoisomers, and an interpretation aided by our theoretical calculations; (5) proposed atmospheric degradation mechanisms and experimentally observed stable end-products, and (6) estimated radiative efficiencies (REs) and GWPs for the individual stereoisomers.

4.1 | OH reaction rate coefficients

4.1.1 | Relative rate (RR) measurements

The relative rate data obtained for the four stereoisomers, (*E*)-2-C₇F₁₄, (*Z*)-2-C₇F₁₄, (*E*)-3-C₇F₁₄, and (*Z*)-3-C₇F₁₄, is displayed in Figure 2 with (*E*)-(CF₃)₂CFCH=CHF (*E*)-HFO-1438ezy) and (*E*)-CF₃CF=CFCF₃ used as the reference compounds. The rate coefficient ratios, k/k_{ref} , were obtained from unweighted linear least-squares fits of the data. The obtained ratios and rate coefficients for reactions 1–4 are given in Table 1. Two experiments were performed for each sample and reference compound by varying reactant concentrations as described in experimental details. The agreement between the individual measurements was within the measurement precision, 1%–5%, obtained from the fits to the data given in Figure 2. The global fit rate coefficient ratios given in Table 1 were obtained from a linear least-squares fit of the combined data. The precision of the individual fits was in the 1%–5% range. The rate coefficients for the (*E*)- isomers were found to be greater than the cor-

responding (*Z*)- isomers with the $k_{(E)}/k_{(Z)}$ ratio being 1.6 for 2-C₇F₁₄ and 2.3 for 3-C₇F₁₄. The agreement between the rate coefficients measured using two reference compounds was in the 8%–10% range, with the rate coefficients measured using the (*E*)-(CF₃)₂CFCH=CHF reference compound being systematically higher. The results from the two reference compounds were averaged to obtain the recommended rate coefficient, k_{rec} . It should be noted that we did not observe evidence for *Z* to *E* isomerization in our experiments.

For determining the absolute uncertainty in the recommended rate coefficients, the measurement precision of k/k_{ref} , the reported uncertainties for the reference compound rate coefficients, and systematic errors in our measurements, GC sampling, and infrared spectra and chromatogram analysis were considered. The recommended rate coefficients with absolute uncertainties are $(3.60 \pm 0.51) \times 10^{-13}$, $(2.22 \pm 0.21) \times 10^{-13}$, $(3.43 \pm 0.47) \times 10^{-13}$, $(1.48 \pm 0.19) \times 10^{-13}$ cm³ molecule⁻¹ s⁻¹ for (*E*)-2-C₇F₁₄, (*Z*)-2-C₇F₁₄, (*E*)-3-C₇F₁₄, and (*Z*)-3-C₇F₁₄, respectively.

4.1.2 | PLP-LIF measurements

Absolute room temperature (296 K) rate coefficients for the reactions of the OH radical with the 2-C₇F₁₄ and 3-C₇F₁₄ stereoisomer mixture samples were measured at 50 and 100 Torr (He bath gas) using a pulsed laser photolysis-laser induced fluorescence (PLP-LIF) technique.¹² The experimental conditions are summarized in the SI. The PLP-LIF measurements provide only an effective rate coefficient for the stereoisomeric mixtures because the C₇F₁₄ samples contain stereoisomers, which have different rate coefficients, as well as unidentified impurities that contribute to k . The obtained effective measured rate coefficient for the 3-C₇F₁₄ sample was $(3.49 \pm 0.03) \times 10^{-13}$ cm³ molecule⁻¹ s⁻¹, where the quoted uncertainty is the 2 σ fit precision (see Figure S7). This is ~3% greater than that obtained from the RR method, 3.39×10^{-13} cm³ molecule⁻¹ s⁻¹, weighted by the stereoisomer sample composition (95.98% (*E*) and 1.18% (*Z*) stereoisomer). The obtained effective rate coefficient for the 2-C₇F₁₄ sample was $(3.90 \pm 0.05) \times 10^{-13}$ cm³ molecule⁻¹ s⁻¹, where the quoted uncertainty is the 2 σ fit precision (see Figure S7). This is ~12% greater than obtained from the stereoisomer weighted RR data (3.43×10^{-13} cm³ molecule⁻¹ s⁻¹) (84.95% (*E*) and 10.82% (*Z*) stereoisomer). The agreement between the PLP-LIF and weighted RR results falls within the combined measurement uncertainties and implies that the unknown impurities did not make a significant contribution to the PLP-LIF rate coefficient measurement.

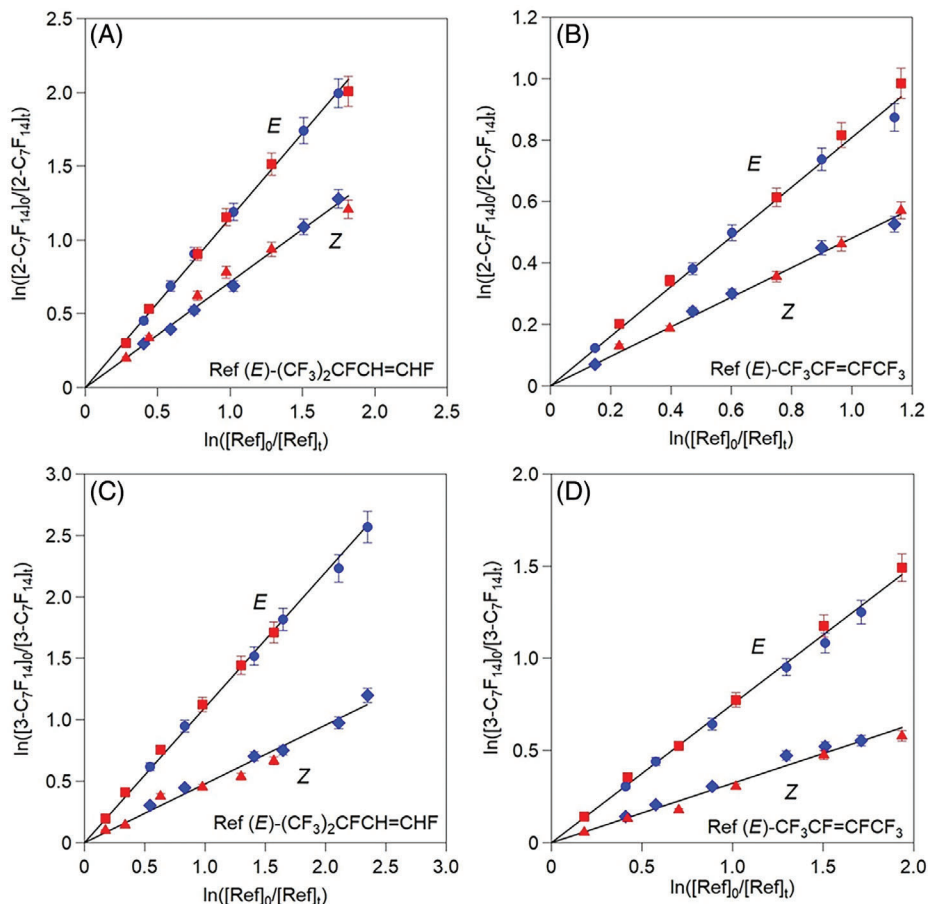


FIGURE 2 OH reaction relative rate (RR) data at 296 K and ~600 Torr (He bath gas) for (*E*)- and (*Z*)- stereoisomers of 2- C_7F_{14} and 3- C_7F_{14} . (A) 2- C_7F_{14} data with (*E*)- $(CF_3)_2CFCH=CHF$ reference. (B) 2- C_7F_{14} data with (*E*)- $CF_3CF=CFCF_3$ reference. (C) 3- C_7F_{14} data with (*E*)- $(CF_3)_2CFCH=CHF$ reference. (D) 3- C_7F_{14} data with (*E*)- $CF_3CF=CFCF_3$ reference. Independent experiments are represented using different symbols. Error bars correspond to 2σ precision of the GC peak height determination. The lines are linear least-squares fits of the combined data sets to Equation (7). The results are summarized in Table 1.

4.2 | O_3 reaction rate coefficients

Rate coefficients, k_{O_3} , for the reaction of ozone (O_3) with 2- C_7F_{14} and 3- C_7F_{14} were measured at 296 K under pseudo-first-order condition in C_7F_{14} , that is, $[O_3] \gg [C_7F_{14}]$ with FTIR detection. k_{O_3} were found to be 3.4×10^{-22} and $2.3 \times 10^{-22} \text{ cm}^3 \text{ molecule}^{-1} \text{ s}^{-1}$ for 2- C_7F_{14} and 3- C_7F_{14} , respectively. The experimental data are provided in SI. O_3 concentration in these experiments was not constant and varied within 20%. Average O_3 concentrations were 3.2×10^{16} and $2.7 \times 10^{16} \text{ molecule cm}^{-3}$ for 2- C_7F_{14} and 3- C_7F_{14} experiments, respectively.

4.3 | Infrared absorption spectra and climate metrics

Infrared absorption spectra for the 2- C_7F_{14} and 3- C_7F_{14} samples recorded in this work are shown in Figures 3

and 4, respectively. Measurements made over a range of sample concentration obeyed Beer's law to better than 2%, see Figures S8 and S9. Digitized spectra are given in the SI. The samples absorb strongly over the wavenumber region 600–1500 cm^{-1} with a strong overlap of the Earth's atmospheric infrared window. The overall congestion of the infrared absorption spectra precludes a quantitative stereoisomer analysis. The integrated band strength of the 2- and 3- C_7F_{14} samples over the 600–1500 cm^{-1} range were measured to be (4.08 ± 0.02) and $(4.03 \pm 0.02) \times 10^{-16} \text{ cm}^2 \text{ molecule}^{-1} \text{ cm}^{-1}$, respectively.

Theoretical calculations of the 2- and 3- C_7F_{14} stereoisomers and their infrared absorption spectra were obtained using DFT as part of this study. The calculated anharmonic band positions and intensities are given in the SI. The calculated spectra are shown in Figure 3, along with the corresponding composition weighted spectra. There is reasonable agreement between the shape and band positions of the experimentally measured and calculated

TABLE 1 Rate coefficients for reactions 1–4 measured in this work using a relative rate (RR) method at 296 K and ~600 Torr (He bath gas).

Compound	Reference: (<i>E</i>)-(CF ₃) ₂ CFCH=CHF		Reference: (<i>E</i>)-CF ₃ CF=CFCF ₃		<i>k</i> _{rec} ^b 10 ⁻¹³ cm ³ molecule ⁻¹ s ⁻¹
	<i>k</i> / <i>k</i> _{ref} ^a	<i>k</i> ^a 10 ⁻¹³ cm ³ molecule ⁻¹ s ⁻¹	<i>k</i> / <i>k</i> _{ref} ^a	<i>k</i> ^a 10 ⁻¹³ cm ³ molecule ⁻¹ s ⁻¹	
(<i>E</i>)-2-C₇F₁₄	1.15 ± 0.02	3.75 ± 0.07	0.79 ± 0.02	3.43 ± 0.09	
	1.14 ± 0.03	3.72 ± 0.10	0.84 ± 0.01	3.65 ± 0.04	
Global fit	1.15 ± 0.02	3.68 ± 0.06	0.81 ± 0.02	3.52 ± 0.07	3.60 ± 0.07
(<i>Z</i>)-2-C₇F₁₄	0.72 ± 0.02	2.35 ± 0.07	0.48 ± 0.02	2.08 ± 0.09	
	0.72 ± 0.05	2.35 ± 0.16	0.49 ± 0.01	2.13 ± 0.04	
Global fit	0.72 ± 0.03	2.35 ± 0.10	0.48 ± 0.01	2.08 ± 0.04	2.22 ± 0.07
(<i>E</i>)-3-C₇F₁₄	1.09 ± 0.04	3.55 ± 0.13	0.77 ± 0.01	3.34 ± 0.04	
	1.12 ± 0.03	3.65 ± 0.10	0.73 ± 0.01	3.17 ± 0.04	
Global fit	1.10 ± 0.03	3.59 ± 0.10	0.75 ± 0.01	3.26 ± 0.04	3.43 ± 0.07
(<i>Z</i>)-3-C₇F₁₄	0.49 ± 0.02	1.60 ± 0.07	0.30 ± 0.01	1.30 ± 0.04	
	0.44 ± 0.02	1.43 ± 0.07	0.34 ± 0.01	1.48 ± 0.04	
Global fit	0.48 ± 0.02	1.56 ± 0.07	0.32 ± 0.01	1.39 ± 0.04	1.48 ± 0.06

^aThe quoted uncertainties are 2σ fit precision values.

^bThe recommended rate coefficient was determined by averaging the results from the two reference compounds (*E*)-(CF₃)₂CFCH=CHF and (*E*)-CF₃CF=CFCF₃.

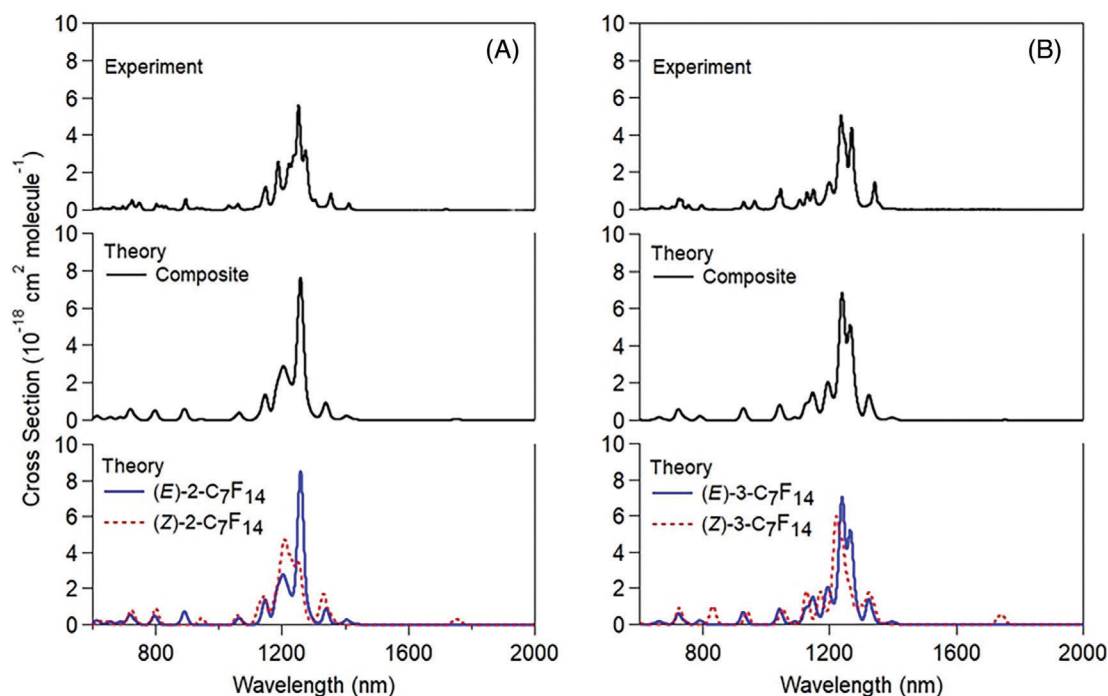


FIGURE 3 (A) 2-C₇F₁₄, (B) 3-C₇F₁₄. Lower panel: theoretical spectra of (*E*) (blue solid trace) and (*Z*) stereoisomers (red dashed trace). Middle panel: theoretical composition weighted composite spectrum. Upper panel: measured infrared spectra.

composition weighted stereoisomer spectra. Although some small band-shifts were observed, the experimentally recorded infrared spectra were reasonably represented by the spectra obtained theoretically, with the latter being used to identify unique bands for each isomer in the samples.

The calculated spectra show that nearly all of the (*E*)- and (*Z*)- stereoisomer bands overlap. For the (*Z*)- stereoisomers, there is a unique band near ~1750 cm⁻¹, however, the intensity of this band is low. The band intensities of the theoretically calculated composite spectra are ~30% greater than the experimentally measured spectra. For the purpose

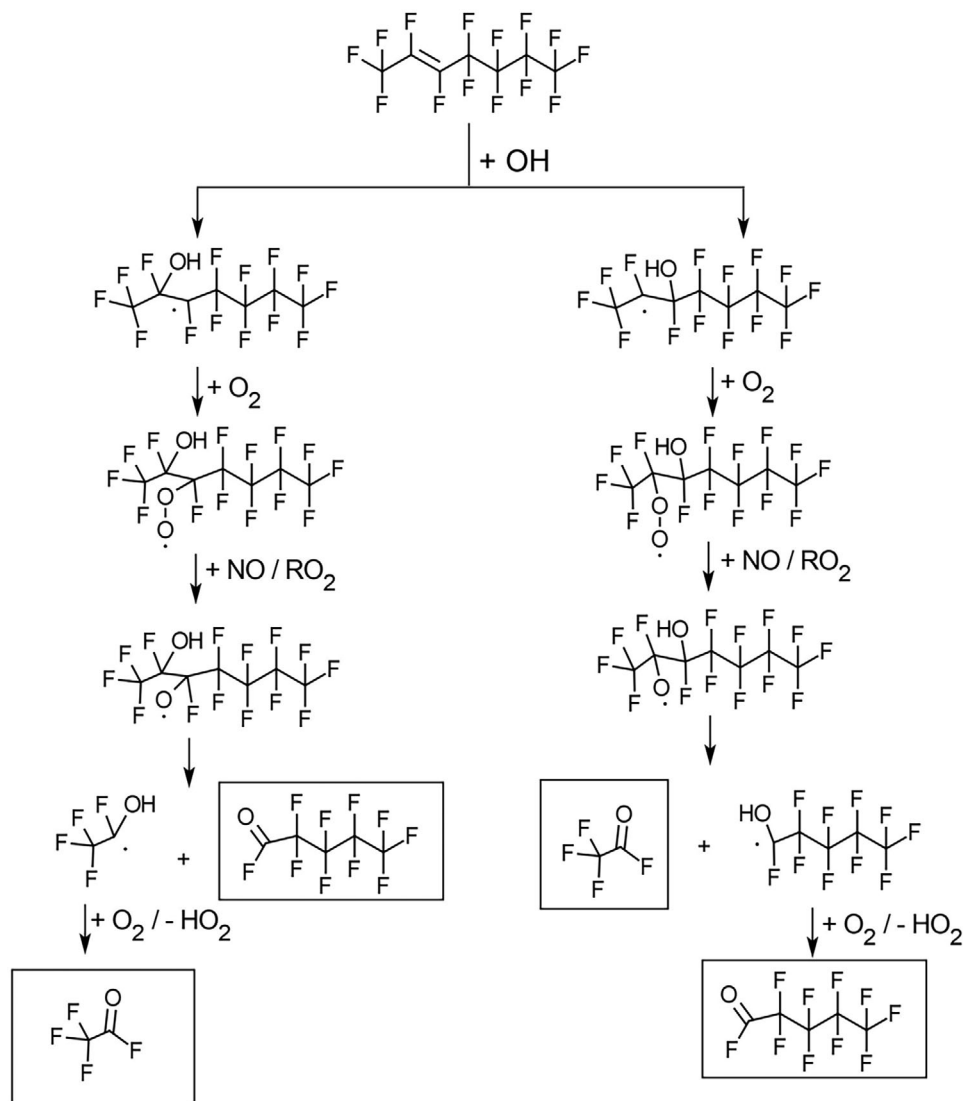


FIGURE 4 Proposed atmospheric degradation mechanism of 2-C₇F₁₄ following reaction with the OH radical.

of calculating stereoisomer specific climate metrics, the calculated spectra were uniformly scaled to agree with the measured integrated band strengths of the 2- and 3-C₇F₁₄ samples between 600 and 1500 cm⁻¹. The well-mixed and adjusted radiative efficiencies of the 2- and 3-C₇F₁₄ theoretically calculated stereoisomers given in Table 2 were determined using the irradiance spectrum in Shine and Myhre.¹³ GWPs for the 100-year time horizon are also given in Table 2.

4.4 | Atmospheric implications

Reaction with OH radical is, most likely, the dominant atmospheric loss process for the 2-C₇F₁₄ and 3-C₇F₁₄. On the basis of the measured rate coefficients for reactions 1–4 in this work the atmospheric lifetime with respect to OH radical reaction for (*E*)-2-C₇F₁₄, (*Z*)-2-C₇F₁₄, (*E*)-

3-C₇F₁₄, (*Z*)-3-C₇F₁₄ are ~33, ~56, ~36, and ~86 days, respectively, for an atmospheric OH radical abundance of 1 × 10⁶ molecule cm⁻³. The magnitude of the atmospheric lifetimes implies possible local to regional environmental impacts.

There are no previous OH kinetic measurements for C₇F₁₄ to compare with the present results. However, the present results can be considered in light of the experimentally measured OH radical rate coefficients for other unsaturated perfluoro compounds, for example, C₂F₄, C₃F₆, 1-C₄F₈, (*E*)-2-C₄F₈, (*Z*)-2-C₄F₈, see Table 3. The OH reactivity of C₇F₁₄ stereoisomers are significantly lower, by one to two orders of magnitude, compared to their C-2 and C-3 homologues for which the measured rate coefficients were 1.0 × 10⁻¹¹ s⁻¹ and 2.2 × 10⁻¹² cm³ molecule⁻¹ s⁻¹, respectively,¹⁵ see Table 3. However, the OH rate coefficients for C₇F₁₄ stereoisomers are only slightly lower than the 2-C₄F₈ isomers indicating that the decrease in

TABLE 2 Lifetimes and climate metrics for the 2-C₇F₁₄ and 3-C₇F₁₄ theoretically calculated stereoisomer infrared spectra obtained in this work.

Molecule	Sample composition	Integrated band strength (10 ⁻¹⁶ cm ² molecule ⁻¹ cm ⁻¹)		Lifetime ^a (days)	Radiative efficiency (well-mixed) (W m ⁻² ppb ⁻¹) ^b	Adjusted radiative efficiency (W m ⁻² ppb ⁻¹) ^c	Global warming potential 100-year time horizon
		Experiment	Theory ^f				
2-C ₇ F ₁₄ Sample ^d		4.08					
(E)-2-C ₇ F ₁₄	84.95%		4.10	32.5	0.49	0.12	1.9
(Z)-2-C ₇ F ₁₄	10.82%		4.35	55.6	0.59	0.19	5.1
3-C ₇ F ₁₄ Sample ^e		4.03					
(E)-3-C ₇ F ₁₄	95.98%		4.11	35.6	0.50	0.12	2.1
(Z)-3-C ₇ F ₁₄	1.18%		4.27	86.4	0.57	0.23	9.3

^aCalculated assuming OH radical reactive loss with [OH] = 1 × 10⁶ molecule cm⁻³.

^bCalculated using the Shine and Myhre¹³ irradiance that includes a molecule dependent stratospheric temperature adjustment.

^cThe adjusted radiative efficiency includes adjustments for the molecules atmospheric lifetime in addition to the stratospheric temperature adjustment.

^dThe 2-C₇F₁₄ Sample also contained 1.72% (E)-3-C₇F₁₄ and 0.79% (Z)-3-C₇F₁₄.

^eThe 3-C₇F₁₄ Sample also contained 1.19% (E)-2-C₇F₁₄ and 0.03% (Z)-2-C₇F₁₄.

^fTheoretical integrated band strengths are scaled downward by 20%–30% to the experimentally measured integrated band strengths between 600 and 1500 cm⁻¹.

TABLE 3 Room temperature OH reaction rate coefficients (*k*_{OH}) for perfluoroalkenes.

Molecule	<i>k</i> _{OH} (10 ⁻¹² cm ³ molecule ⁻¹ s ⁻¹)	References
C ₂ F ₄	10.0	Orkin et al. ¹⁴
C ₃ F ₆	2.2	Orkin et al. ¹⁵
1-C ₄ F ₈	1.9	Young et al. ¹⁶
(E)-2-C ₄ F ₈	0.43	Baasandorj et al. ³
(Z)-2-C ₄ F ₈	0.33	Baasandorj et al. ³
(E)-2-C ₇ F ₁₄	0.36	This study
(Z)-2-C ₇ F ₁₄	0.22	This study
(E)-3-C ₇ F ₁₄	0.34	This study
(Z)-3-C ₇ F ₁₄	0.15	This study

the rate coefficients with the increase in carbon chain length becomes less significant. The measured rate coefficient for the (E)- stereoisomer of C₄F₈ was found to be greater than that for the (Z)- stereoisomer, which is consistent with the measurements carried out for C₇F₁₄ in this work.³

A proposed atmospheric degradation mechanism for 2-C₇F₁₄ and 3-C₇F₁₄ following OH radical addition reaction is given in Figure 4 and Figure S11, respectively. For both 2-C₇F₁₄ and 3-C₇F₁₄, OH can add from two opposite sides of >C=C< double bond. The carbon centered radical reacts with O₂ present in the atmosphere forming a peroxy (RO₂) radical. The peroxy (RO₂) radical reacts with NO to form alkoxy (RO) radicals. Reaction with RO₂ and HO₂ radicals under some conditions in the atmosphere are also possible. The alkoxy radicals are

expected to lead to the formation of stable carbonyl end-products. The expected carbonyl end-products for 2-C₇F₁₄ are CF₃C(O)F and C₄F₉C(O)F. These fluorocarbonyl products are expected to be formed in a 1:1 yield for both of the possible OH addition channels. For 3-C₇F₁₄, the stable end-products are C₂F₅C(O)F and C₃F₇C(O)F. The atmospheric fate of all of these perfluorocarbonyl end products is expected to be heterogeneous hydrolysis to form perfluoro-acids.

A OH reaction products study was performed at ~615 Torr (syn. air) and 296 K. Figure 5 shows the product yields as a function of the 2-C₇F₁₄ loss. The corresponding data for 3-C₇F₁₄ is given in Figure S12. CF₃C(O)F was observed as a major primary product of the OH + 2-C₇F₁₄ reaction. The infrared spectrum of CF₃C(O)F was recorded previously in our laboratory¹⁷ and was used to quantify CF₃C(O)F. The secondary loss of CF₃C(O)F, due to 248 nm photolysis and hydrolysis on the system surfaces, led to a non-linear yield for CF₃C(O)F. On the basis of the initial production of CF₃C(O)F, its molar yield was estimated to be ~98%. The near unity yield of CF₃C(O)F is consistent with the reaction mechanism proposed in Figure 4. Infrared absorption spectrum of C₄F₉C(O)F has not been reported in the literature to date. The C₄F₉C(O)F product yield was also non-linear. We assume a C₄F₉C(O)F yield similar to that of CF₃C(O)F, that is, unity, see Figure 5. CF₂O, CO, and CO₂ were observed as secondary products. Infrared absorption cross sections for CF₂O, CO, and CO₂ were taken from the PNNL database¹⁸ to quantify these products. Based on the measured and assumed product yields, the carbon mass balance was calculated to be ~1.1.

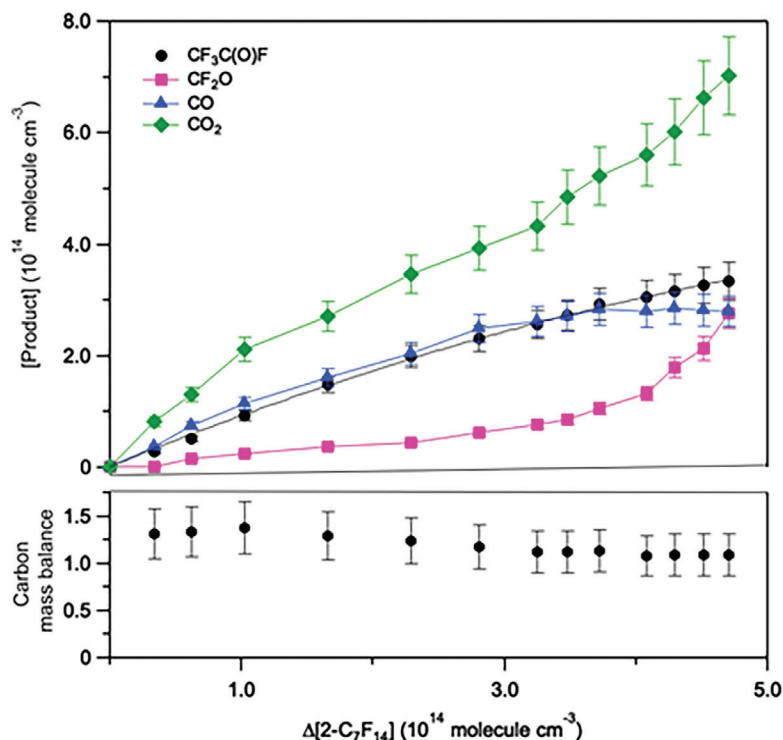


FIGURE 5 Stable end-product formation following the OH initiated oxidation of 2- C_7F_{14} at 296 K in 615 Torr (syn. air). The initial 2- C_7F_{14} concentration was 6.2×10^{14} molecule cm^{-3} . The line for $CF_3C(O)F$ is an empirical second order polynomial fit. Other lines through data points are for guiding purpose only. The error bars a 2σ measurement precision. The lower panel shows the carbon mass balance assuming $[C_4F_9C(O)F] = [CF_3C(O)F]$ throughout the experiment.

5 | CONCLUSION

The atmospherically relevant OH radical + 2-perfluoroheptene (2- C_7F_{14}) and 3-perfluoroheptene (3- C_7F_{14}) reactions were studied in this work at 296 K. The reaction with the OH radical is considered to be the major gas-phase loss process of these compounds in the atmosphere. OH reaction rate coefficients for individual perfluoroheptene stereoisomers were experimentally measured using a relative rate method from samples containing a mixture of stereoisomers. OH reaction rate coefficients at 296 K and ~ 600 Torr (He bath gas) were measured to be $(3.60 \pm 0.51) \times 10^{-13}$, $(2.22 \pm 0.21) \times 10^{-13}$, $(3.43 \pm 0.47) \times 10^{-13}$, and $(1.48 \pm 0.19) \times 10^{-13}$ cm^3 molecule $^{-1}$ s $^{-1}$ for (*E*)-2- C_7F_{14} , (*Z*)-2- C_7F_{14} , (*E*)-3- C_7F_{14} , and (*Z*)-3- C_7F_{14} , respectively. The atmospheric lifetimes determined from the OH rate coefficients are ~ 33 , ~ 56 , ~ 36 , and ~ 86 days, for (*E*)-2- C_7F_{14} , (*Z*)-2- C_7F_{14} , (*E*)-3- C_7F_{14} , (*Z*)-3- C_7F_{14} , respectively. Rate coefficients for the (*E*)- stereoisomers were found to be greater than that of the corresponding (*Z*)- stereoisomers, which is consistent with the previously measured rate coefficients for the C_4F_8 stereoisomers.³ However, the data base for (*E*) and (*Z*) reactivity for perfluoroolefins is too limited to infer a reactivity trend. An atmospheric degradation mechanism for C_7F_{14} following OH radical addition was presented. The stable end products are expected to be perfluorocarbonyl compounds. The atmospheric fate of the perfluoro aldehyde end-products in the oxidation of 2- and 3- C_7F_{14} is, most likely, wet deposition and hydrolysis

to form perfluoro acids. The perfluoro acids would rain out and enter the hydrosphere.

ACKNOWLEDGMENTS

We thank Chemours for providing the samples used in this work. This work was supported in part by NOAA's Climate Program Office Atmospheric Chemistry, Carbon Cycle, and Climate Program and NASA's Atmospheric Composition Program.

CONFLICT OF INTEREST STATEMENT

No, there is no conflict of interest to disclose.

DATA AVAILABILITY STATEMENT

The data that supports the findings of this study are available in the supplementary material of this article.

ORCID

Aparajeo Chattopadhyay  <https://orcid.org/0000-0003-0063-6685>

Vassileios C. Papadimitriou  <https://orcid.org/0000-0002-8299-4306>

James B. Burkholder  <https://orcid.org/0000-0001-9532-6246>

REFERENCES

- Burkholder JB, Cox RA, Ravishankara AR. Atmospheric degradation of ozone depleting substances, their substitutes, and related species. *Chem Rev.* 2015;115:3704-3759.

- Jubb AM, Gierczak T, Baasandorj M, Waterland RL, Burkholder JB. Methyl-perfluoroheptene-ethers ($\text{CH}_3\text{OC}_7\text{F}_{13}$): measured OH radical reaction rate coefficients for several isomers and enantiomers and their atmospheric lifetimes and global warming potentials. *Environ Sci Technol*. 2014;48:4954-4962.
- Baasandorj M, Papadimitriou VC, Burkholder JB. Rate coefficients for the gas-phase reaction of (*E*)- and (*Z*)- $\text{CF}_3\text{CF}=\text{CFCF}_3$ with the OH radical and Cl-atom. *J Phys Chem A*. 2019;123:5051-5060.
- Baasandorj M, Marshall P, Waterland RL, Ravishankara AR, Burkholder JB. Rate coefficient measurements and theoretical analysis of the OH + (*E*)- $\text{CF}_3\text{CH}=\text{CHCF}_3$ reaction. *J Phys Chem A*. 2018;122:4635-4646.
- Baasandorj M, Ravishankara AR, Burkholder JB. Atmospheric chemistry of (*Z*)- $\text{CF}_3\text{CH}=\text{CHCF}_3$: OH radical reaction rate coefficient and global warming potential. *J Phys Chem A*. 2011;115:10539-10549.
- Gierczak T, Baasandorj M, Burkholder JB. OH + (*E*)- and (*Z*)-1-Chloro-3,3,3-trifluoropropene-1 ($\text{CF}_3\text{CH}=\text{CHCl}$) reaction rate coefficients: stereoisomer-dependent reactivity. *J Phys Chem A*. 2014;118:11015-11025.
- Tokuhashi K, Uchimaru T, Takizawa K, Kondo S. Rate constants for the reactions of OH radicals with the (*E*)/(*Z*) isomers of $\text{CFCl}=\text{CFCl}$ and (*E*)- $\text{CHF}=\text{CHF}$. *J Phys Chem A*. 2019;123:4834-4843.
- Tokuhashi K, Takizawa K, Kondo S. Rate constants for reactions of OH radicals with (*Z*)- $\text{CF}_3\text{CCl}=\text{CHCl}$, $\text{CHF}_2\text{CF}=\text{CF}_2$, (*E*)- $\text{CF}_3\text{CH}=\text{CHF}$, (*Z*)- $\text{CF}_3\text{CH}=\text{CHF}$, $\text{CH}_3\text{CF}=\text{CH}_2$, and $\text{CH}_2\text{FCH}=\text{CH}_2$. *Atmos Environ*. 2021;255:118428.
- Hurley MD, Ball JC, Wallington TJ. Atmospheric chemistry of the *Z* and *E* isomers of CF_3CFCHF ; kinetics, mechanisms, and products of gas-phase reactions with Cl atoms, OH radicals, and O_3 . *J Phys Chem A*. 2007;111:9789-9795.
- Chattopadhyay A, Gierczak T, Marshall P, Papadimitriou VC, Burkholder JB. Kinetic fall-off behavior for the Cl + Furan-2,5-dione ($\text{C}_4\text{H}_2\text{O}_3$, maleic anhydride) reaction. *Phys Chem Chem Phys*. 2021;23:4901-4911.
- Papadimitriou VC, Burkholder JB. OH radical reaction rate coefficients, infrared spectrum, and global warming potential of (CF_3)₂ $\text{CFCH}=\text{CHF}$ (HFO-1438ezy(*E*)). *J Phys Chem A*. 2016;120:6618-6628.
- Chattopadhyay A, Papadimitriou VC, Marshall P, Burkholder JB. Temperature-dependent rate coefficients for the gas-phase OH + furan-2,5-dione ($\text{C}_4\text{H}_2\text{O}_3$, maleic anhydride) reaction. *Int J Chem Kinet*. 2020;52:623-631.
- Shine KP, Myhre G. The spectral nature of stratospheric temperature adjustment and its application to halocarbon radiative forcing. *J Adv Model Earth Syst*. 2020;12:e2019MS001951.
- Orkin VL, Louis F, Huie RE, Kurylo MJ. Photochemistry of bromine-containing fluorinated alkenes: reactivity toward OH and UV spectra. *J Phys Chem A*. 2002;106:10195-10199.
- Orkin VL, Poskrebyshev GA, Kurylo MJ. Rate constants for the reactions between OH and perfluorinated alkenes. *J Phys Chem A*. 2011;115:6568-6574.
- Young CJ, Hurley MD, Wallington TJ, Mabury SA. Atmospheric chemistry of perfluorobutenes (CF_3CFCF_3 and $\text{CF}_3\text{CF}_2\text{CFCF}_2$): kinetics and mechanisms of reactions with OH radicals and chlorine atoms, IR spectra, global warming potentials, and oxidation to perfluorocarboxylic acids. *Atmos Environ*. 2009;43:3717-3724.
- Papadimitriou VC, Lazarou YG, Talukdar RK, Burkholder JB. Atmospheric chemistry of $\text{CF}_3\text{CF}=\text{CH}_2$ and (*Z*)- $\text{CF}_3\text{CF}=\text{CHF}$: Cl and NO_3 rate coefficients, Cl reaction product yields, and thermochemical calculations. *J Phys Chem A*. 2011;115:167-181.
- Sharpe SW, Johnson TJ, Sams RL, Chu PM, Rhoderick GC, Johnson PA. Gas-phase databases for quantitative infrared spectroscopy. *Appl Spectrosc*. 2004;58:1452-1461.

SUPPORTING INFORMATION

Additional supporting information can be found online in the Supporting Information section at the end of this article.

How to cite this article: Chattopadhyay A, Papadimitriou VC, Burkholder JB. OH reaction rate coefficients, infrared spectra, and climate metrics for (*E*)- and (*Z*)- 2-perfluoroheptene (2- C_7F_{14}) and 3-perfluoroheptene (3- C_7F_{14}). *Int J Chem Kinet*. 2023;55:392-401. <https://doi.org/10.1002/kin.21643>